Journal of Luminescence 152 (2014) 145–147

Contents lists available at ScienceDirect

Journal of Luminescence

journal homepage: www.elsevier.com/locate/jlumin

Near-infrared luminescence characteristics of Yb^{3+}- and Er^{3+}-codoped $NaYS_2$ powder material

Jisen Zhang *, Liguo Zhang, Jianyue Ren, Liping Zhang, Yongshi Luo, Shaozhe Lü

Changchun Institute of Optics, Fine Mechanics and Physics, Chinese Academy of Sciences, 3888 Dongnanhu Road, Changchun 130033, PR China

ARTICLE INFO

Available online 25 December 2013

Keywords:
Rare earth ions
NIR luminescence
Charge-transfer state

ABSTRACT

Yb^{3+}- and Er^{3+}-doped $NaYS_2$: powder samples were synthesized with solid-state reacting method, and the near-infrared luminescence characters of Er^{3+} were presented with the spectra obtained following an excitation at 980 nm or 532 nm, respectively. Exploring dependences of the relative emission intensities on excited power density, Er^{3+}-doped content and S^{2-}–Re^{3+} (Re^{3+} standing for Yb^{3+} or Er^{3+}) charge transfer state, the mechanism of the energy-transfer processes between Yb^{3+} and Er^{3+} would be suggested with a schematic energy-level scheme based on the energy matching conditions.

1. Introduction

It has been well known that the infrared (IR) luminescence of rare-earth ions (Re^{3+}) is very weak due to upconversion effect, nonradiative relaxation between narrow levels and low *f–f* absorption cross-section. However, Re^{3+}-codoped phosphors which shows sufficiently strong IR luminescence under laser excitation on 900–980 nm have been developed [1] and, specially the near-infrared (NIR) emissions of Er^{3+} at 1540 nm or 808 nm have attracted much attention in a wide variety of applications such as planar waveguide amplifiers, plastic lasers and luminescent probes, and so on in recent two decade years [2–5]. Some work indicated that Ce^{3+} was able to selectively sensitize the NIR luminescence with Er^{3+} in the ranges of 1500–1600 nm and quench the visible upconversion luminescence [6–8] and, by doping transition-metal ions [9] or introducing organic ligands [10] into complexes of Er^{3+}, the NIR-emitting quantum yield of Er^{3+} was effectively improved on the basis of energy-transfer processes. In recent years, based on the energy position of charge-transfer state (CTS) being related to the element and structure of hosts [11–15] in the Re^{3+}-doped materials, it was found that the S^{2-}(sulfur ion)–Yb^{3+} CTS can make it competitive with $^4F_{9/2}$, $^2H_{11/2}$ and $^4S_{3/2}$ emission of Er^{3+}, decreasing their population and quenching the visible emissions in a Er^{3+}–Yb^{3+}-codoped phonon-energy-low sulfide host [16].

Here, the NIR luminescence characteristics of Er^{3+}–Yb^{3+}-codoped $NaYS_2$: powder material was researched by using the emission spectra following an excitation, respectively, at 980 nm or 532 nm at room temperature. By researching the dependences of the NIR emission intensities on the excited power density and the excitation wavelength, a schematic energy-level scheme was used to well explained the energy-transfer processes in the Re^{3+}-doped material with the S^{2-}–Yb^{3+} CTS based on the energy matching conditions.

2. Experiments

The synthesis of $NaYS_2$: $0.20Yb^{3+}$, $0.03Er^{3+}$ powder sample was based on a co-precipitation method and a calcining procedure [6]. The original materials, such as $YCl_3 \cdot 6H_2O$, $YbCl_3 \cdot 6H_2O$, $ErCl_3 \cdot 6H_2O$, and Na_2S were all analytical reagents. First, by $4Na_2S + 2YCl_3 = 2NaYS_2 + 6NaCl$, stoichiometric $YCl_3 \cdot 6H_2O$, $YbCl_3 \cdot 6H_2O$ and $ErCl_3 \cdot 6H_2O$ was dissolved together in distilled water at room temperature to form clear solution, and Na_2S (10% overweight) was dissolved in other a beaker. Then the two solutions were mixed to form colloidal solution while stirring with a magnetic stirrer. The solution was concentrated by using electric cooker and the remainder was dried at 150 °C for 3 h. After calcined at 1000 °C for 2 h in a sulfur atmosphere, the powder sample was obtained

XRD analysis was carried out with Rigaku RU-200b powder diffractometer using Ni-filtered Cu*K*α radiation with $\lambda = 0.15406$ nm. Emission spectra were recorded with Triax550 spectrometer from JY. All measurements were performed at room temperature.

3. Results and discussion

First, the XRD pattern of $NaYS_2$:$0.20Yb^{3+}$, $0.03Er^{3+}$ sample is displayed in Fig. 1 at room temperature, which shows a rhombohedral

* Corresponding author. Tel.: +86 43186708850; fax: +86 43186176317.
E-mail address: zhangjisen1962@163.com (J. Zhang).

0022-2313/$ - see front matter © 2013 Elsevier B.V. All rights reserved.
http://dx.doi.org/10.1016/j.jlumin.2013.12.002

$NaYS_2$ phase with the space group *R*3*m* comparing with the standard data of $NaYS_2$ crystal (JCPDS 46-1051).

Fig. 2 displays the emission spectra of $NaYS_2$:0.20Yb^{3+}, 0.03Er^{3+} powder following an excitation at 980 nm with different excitation power, respectively. It is obvious that the emission spectra are very different from that in Er^{3+}–Yb^{3+}-codoped oxide [17] or fluoride [18] hosts. As shown in Fig. 2, the NIR emission at 830 nm is broadened and the most prominent one in Fig. 2(a). Comparing Fig. 2(a) with (b), the phenomenon can only be maintained under correspondingly the low excitation power. At the same time the visible emission from $^4S_{3/2}$ and $^2H_{11/2}\rightarrow{}^4I_{15/2}$ is always weak and the emission intensity of $^4F_{9/2}\rightarrow{}^4I_{15/2}$ and $^4I_{13/2}\rightarrow{}^4I_{15/2}$ shows an increase with increasing the excitation power, respectively.

Fig. 3 shows the emission spectrum of $NaYS_2$:0.20Yb^{3+}, 0.03Er^{3+} sample following an excitation at 532 nm. As shown in Fig. 3, a monospectral NIR light-emitting due to the radiation transitions from $^4I_{9/2}\rightarrow{}^4I_{15/2}$ is identified. Comparing with the spectra in Fig. 2, only prominent band-narrower luminescence in the ranges of 800–820 nm is obtained under the excitation at 532 nm while the emissions, such as the visible radiation transitions of $^4S_{3/2}\rightarrow{}^4I_{15/2}$, $^4F_{9/2}\rightarrow{}^4I_{15/2}$ and the NIR radiation transition of $^4I_{13/2}\rightarrow{}^4I_{15/2}$ are missing.

To understand the mechanism of the NIR emissions and the energy-transfer processes between Yb^{3+} and Er^{3+} in $NaYS_2$: 0.20Yb^{3+}, 0.03Er^{3+} powder, a schematic energy-level diagram is proposed based on the features above. It is suggested that the effects of S^{2-}–Yb^{3+} CTS would play a key role in the NIR luminescence of Er^{3+} in $NaYS_2$:0.20Yb^{3+}, 0.03Er^{3+} sample.

As described in Fig. 4, the $^4F_{7/2}$ level of Er^{3+} could be primarily populated by absorbing two 980-nm photons with the energy-transfer processes from Yb^{3+} to Er^{3+}, simultaneously making the S^{2-}–Er^{3+} CTS done because the $^4F_{7/2}$ level is covered with the S^{2-}–Er^{3+} CTS here. Then $^4S_{3/2}$ level can be populated with nonradiative relaxation process from S^{2-}–Er^{3+} CTS to $^2H_{11/2}$ to $^4S_{3/2}$. And further the nonradiative relaxation process from $^4S_{3/2}$ to S^{2-}–Er^{3+} CTS to $^4I_{9/2}$ could occur with the interaction between Er^{3+} and Yb^{3+} and the S^{2-}–Yb^{3+} CTS, leading to the $^4I_{9/2}$ being populated last. As shown in Fig. 1(a), it is evident that the radiation transition from $^4F_{9/2}$ to $^4I_{15/2}$ always is weak, which would be attributed to the negligible interaction between the excited Er^{3+} ions in the doped Er^{3+} amount under a low excitation power, resulting in the $^4F_{9/2}$ level being not efficiently populated. So the strong NIR emission peaked at 830 nm due to the transition from $^4I_{9/2}$ to $^4I_{15/2}$ can is gained under a low excitation power. However, the interaction between the excited Er^{3+} ions must be considered due to the excited Er^{3+} amount increase with increasing the 980-nm excitation power, the $^4F_{9/2}$ level can be efficiently populated with the cross-relaxation process of ($^4I_{9/2}$, $^4I_{11/2}$)→($^4F_{9/2}$,

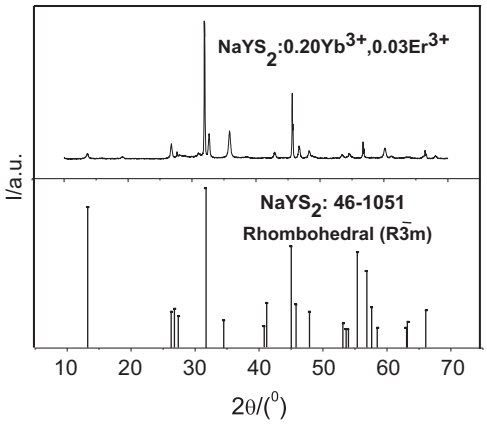

Fig. 1. XRD pattern of $NaYS_2$:0.20Yb^{3+}, 0.03Er^{3+} and standard $NaYS_2$ sample.

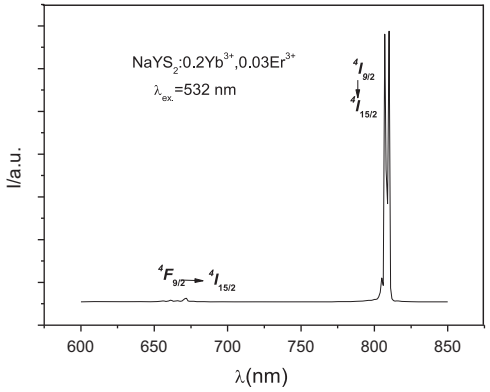

Fig. 3. Emission spectra of $NaYS_2$: 0.20Yb^{3+}, 0.03Er^{3+} sample following an excitation at 532 nm.

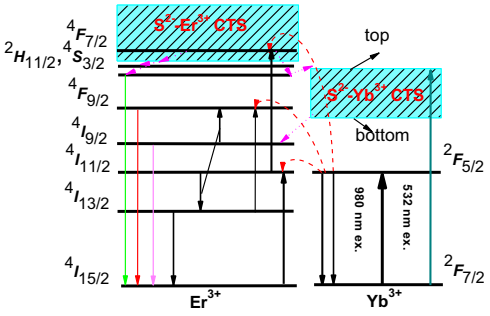

Fig. 4. Energy-transfer processes between Yb^{3+} and Er^{3+} in $NaYS_2$: 0.20Yb^{3+}, 0.03Er^{3+} sample at room temperature.

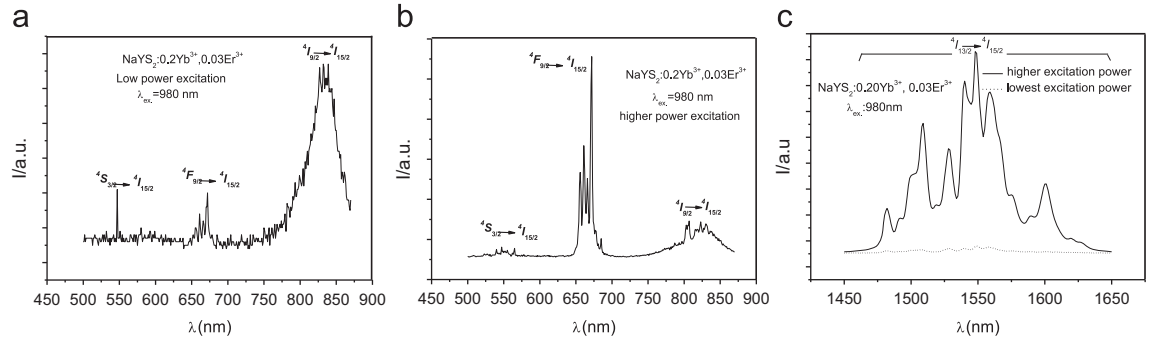

Fig. 2. Emission spectra of $NaYS_2$:0.20Yb^{3+}, 0.03Er^{3+} sample following an excitation at 980 nm.

$^4I_{13/2}$) and the transition of $^4I_{13/2} \rightarrow {}^4F_{9/2}$ by absorbing a 980-nm photon. In fact, as shown in Fig. 1(b) the emission of $^4F_{9/2} \rightarrow {}^4I_{15/2}$ become strongest under a higher 980-nm excitation power. At the same time as seen in Fig. 2(c), the NIR radiation transition of $^4I_{13/2} \rightarrow {}^4I_{15/2}$ always increases with increasing 980-nm excitation power because of the cross-relaxation process of ($^4I_{9/2}$, $^4I_{11/2}$)→($^4F_{9/2}$, $^4I_{13/2}$). In addition, based to S^{2-}–Yb^{3+} CTS being able to absorb 532-nm photons more efficiently as shown in Fig. 4, the population of $^4I_{9/2}$ can be achieved with the nonradiative relaxation process from S^{2-} to Yb^{3+} CTS to $^4I_{9/2}$ level, leading to a strong NIR emission at 815 nm observed exclusively.

4. Conclusions

In conclusion, our experimental results have demonstrated that not only the NIR emission can be obtained under a low 980-nm excitation power but also a strong monospectral NIR emission can be observed under 532-nm excitation in the range of 800–900 nm in $NaYS_2$:0.20Yb^{3+}, 0.03Er^{3+} powder, which makes it more attractive for applications in biological and medical fields because the minimal absorbency in the human body is in the ranges of 700–900 nm [19,20]. Further it is identified that the dominant reasons giving rise to the efficient NIR emissions with Er^{3+} would be the energy position of S^{2-}–Yb^{3+} CTS following an excitation at 980 nm or 532 nm in the $NaYS_2$:0.20Yb^{3+}, 0.03Er^{3+} material. It is revelatory for the experimental results to be devoted to the search for novel NIR phosphors.

Acknowledgments

The authors would like to appreciate the support of the National Natural Science Foundation of China under Grant Nos. 11174276 and 11174278.

References

[1] F. Auzel, Chem. Rev. 104 (2004) 139.
[2] L.H. Slooff, A. Van Blaaderen, A. Polman, G.A. Hebbink, S.I. Klink, F.C.J.M. van Veggel, D.N. Reinhoudt, J.W. Hofstraat, J. Appl. Phys. 91 (2002) 3955.
[3] Z.F. Krasilnik, B.A. Andreev, D.I. Kryzhkov, L.V. Krasilnikova, V.P. Kuznetsov, D.Y. Remizov, V.B. Shmagin, M.V. Stepikhova, A.N. Yablonskiy, T. Gregorkievicz, N.Q. Vinh, W. Jantsch, H. Przybylinska, V.Y. Timoshenko, D.M. Zhigunov, J. Mater. Res. 21 (2006) 574.
[4] C. Bader, I. Krejci, Am. J. Dent. 19 (2006) 178.
[5] Jisen Zhang, Liguo Zhang, Jianyue Ren, et al., Chin. J. Lumin. 34 (2013) 542.
[6] L. Su, J Xu, H. Li, et al., J. Lumin. 122–123 (2007) 17.
[7] A.N. Georgobiani, V.B. Gutan, M.A. Kazaryan, A.V. Krotova, O.Ya. Manashirov, Yu.P. Timofeev, Inorg. Mater. 45 (2009) 1166.
[8] Jian Xin Meng, Jin Qing Li, Zhao Pu Shi, Kok Wai Cheah, Appl. Phys. Lett. 93 (2008) 221908.
[9] D.W. Michael, Coord. Chem. Rev. 251 (2007) 1663.
[10] Nam Seob Baek, Bong Kyu Kwak, Yong Hee Kim, Hwan Kyu Kim, Bull. Korean Chem. Soc. 28 (2007) 1256.
[11] Hongpeng You, Guangyan Hong, Xiaoqing Zeng, C.-H. Kim, C.-H. Pyun, B.-Y. Yu, H.-S. Bae, J. Phys. Chem. Solids 61 (2000) 1985.
[12] H.E. Hoefdraad, J. Solid State Chem. 15 (1975) 175.
[13] G. Blasse, J. Chem. Phys. 45 (1966) 2356.
[14] Ling Li, Siyuan Zhang, J. Phys. Chem. B 110 (2006) 21438.
[15] L.J. Nugent, R.D. Baybarz, J.L. Burnett, J. Phys. Chem. 73 (1969) 1177.
[16] Pascal Gerner, Hans U. Güdel, Chem. Phys. Lett. 413 (2005) 105.
[17] Ying Yu, Dawei Qi, Hua Zhao, J. Lumin. 143 (2013) 388.
[18] S. Gorgescu, A.M. Viculescu, C. Matei, C.B. Secu, R.F. Negrea, M. Secu, J. Lumin. 143 (2013) 150.
[19] M.E. Daub, M. Ehrenshaft, Annu. Rev. Phytopathol. 38 (2000) 461.
[20] K. Licha, C. Olbrich, Adv. Drug Delivery Rev. 57 (2005) 1087.